JB
Journals.ASM.org

# Steady-State Hydrogen Peroxide Induces Glycolysis in *Staphylococcus aureus* and *Pseudomonas aeruginosa*

**Xin Deng,[a] Haihua Liang,[a] Olesya A. Ulanovskaya,[b,c] Quanjiang Ji,[a] Tianhong Zhou,[a] Fei Sun,[a] Zhike Lu,[a] Alan L. Hutchison,[a] Lefu Lan,[d] Min Wu,[e] Benjamin F. Cravatt,[b,c] Chuan He[a]**

Department of Chemistry and Institute for Biophysical Dynamics, The University of Chicago, Chicago, Illinois, USA[a]; The Skaggs Institute for Chemical Biology, The Scripps Research Institute, La Jolla, California, USA[b]; Department of Chemical Physiology, The Scripps Research Institute, La Jolla, California, USA[c]; Shanghai Institute of Materia Medica, Chinese Academy of Sciences, Pudong Zhangjiang Hi-Tech Park, Shanghai, China[d]; Department of Biochemistry and Molecular Biology, University of North Dakota, Grand Forks, North Dakota, USA[e]

**Glyceraldehyde-3-phosphate dehydrogenase (GAPDH) from human pathogens *Staphylococcus aureus* and *Pseudomonas aeruginosa* can be readily inhibited by reactive oxygen species (ROS)-mediated direct oxidation of their catalytic active cysteines. Because of the rapid degradation of $H_2O_2$ by bacterial catalase, only steady-state but not one-dose treatment with $H_2O_2$ rapidly induces glycolysis and the pentose phosphate pathway (PPP). We conducted transcriptome sequencing (RNA-seq) analyses to globally profile the bacterial transcriptomes in response to a steady level of $H_2O_2$, which revealed profound transcriptional changes, including the induced expression of glycolytic genes in both bacteria. Our results revealed that the inactivation of GAPDH by $H_2O_2$ induces metabolic levels of glycolysis and the PPP; the elevated levels of fructose 1,6-biphosphate (FBP) and 2-keto-3-deoxy-6-phosphogluconate (KDPG) lead to dissociation of their corresponding glycolytic repressors (GapR and HexR, respectively) from their cognate promoters, thus resulting in derepression of the glycolytic genes to overcome $H_2O_2$-stalled glycolysis in *S. aureus* and *P. aeruginosa*, respectively. Both GapR and HexR may directly sense oxidative stresses, such as menadione.**

Pathogenic bacteria, such as *Pseudomonas aeruginosa* and *Staphylococcus aureus*, need to conquer high concentrations of reactive oxygen species (ROS) that are produced by host phagocytic cells for sustained virulence (1). To this end, these bacteria use ROS-reactive small molecules, such as glutathione (GSH) and melanin in *P. aeruginosa* as well as coenzyme A and staphyloxanthin in *S. aureus*. These pathogens also produce a group of ROS-detoxifying enzymes, such as catalase, superoxide dismutase, hydroperoxide reductase, thioredoxin, and glutaredoxin, whose expression is induced by oxidative stress (2–4).

It has been well documented that *P. aeruginosa* and *S. aureus* also mount global transcriptional changes by utilizing a group of thiol-based ROS-active transcription regulators, such as OxyR, SoxR, MgrA, OhrR, SarA, SarZ, MexR, OspR, CymR, AirSR, and AgrA (5–15). Upon oxidative stress, the specific cysteine groups in these regulatory proteins form sulfenic acids or disulfides, thus inducing conformational changes that attenuate their DNA binding affinities. Our previous work showed that a thiol-based, oxidation-sensing mechanism is utilized by these human pathogens to sense the host immune response and regulate a global change of their properties. ROS leads to activation of defense systems to reduce the oxidative threat as well as a major shift in the life forms of the pathogens (6, 11).

ROS can efficiently oxidize the thiol group of active and allosteric cysteines in bacterial proteins, causing changes in their functions. Previously, we employed an isotopic orthogonal proteolysis–activity-based protein profiling (isoTOP-ABPP) technology to identify around 200 oxidation-sensitive cysteines and further determined that several of these proteins perform important redox-active functions in bacteria. The master quorum sensing regulator LasR of *P. aeruginosa* undergoes an oxidation-responsive transcriptional regulation. Oxidation induces switching of metabolic pathways by modification of active site and/or allosteric cysteine residues in enzymes, such as acetaldehyde dehydrogenase ExaC, arginine deiminase ArcA, and glyceraldehyde-3-phosphate dehydrogenase (GAPDH) (16). GAPDH is readily oxidized and inhibited by oxidation. Pathogenic bacteria exhibit a complex, multilayer response to ROS that includes the rapid adaption of metabolic pathways to oxidative stress challenge (17).

Central metabolism has profound influences on bacterial response to ROS. The pentose phosphate pathway (PPP) contributes bacterial tolerance to oxidative stress by generating the redox currency (NADPH), which is the substrate for other reducing agents (18). NADPH is responsible for generating glutathione (GSH) in *P. aeruginosa* and reduced thioredoxin in *S. aureus* (19, 20). In addition, PPP is important for producing nucleotide precursors to repair DNA damage under ROS stress in *Deinococcus radiodurans* (21), suggesting a potentially conserved mechanism in other bacteria. In *S. aureus*, PPP is linked with glycolysis, which is strictly regulated by the glycolytic repressor GapR (22). In *Bacillus subtilis*, fructose 1,6-biphosphate (FBP) is the cognate ligand that derepresses CggR, the ortholog of GapR (23), suggesting a similar interaction between FBP and GapR in *S. aureus*. In *P. aeruginosa*, PPP is closely associated with the Entner-Doudoroff (ED) pathway, which is controlled by the repressor HexR. HexR specifically senses 2-keto-3-deoxy-6-phosphogluconate (KDPG),

**Received** 5 February 2014 **Accepted** 22 April 2014
**Published ahead of print** 25 April 2014
Address correspondence to Chuan He, chuanhe@uchicago.edu.
Supplemental material for this article may be found at http://dx.doi.org/10.1128/JB.01538-14.

doi:10.1128/JB.01538-14

which results in derepression of several ED operons (24). It has been shown in yeast (*Saccharomyces cerevisiae*) that upon ROS, oxidative inhibition of glyceraldehyde-3-phosphate dehydrogenase (GAPDH) leads to prompt metabolic redirection from glycolysis to PPP, which generates more NADPH (25). However, a similar GAPDH-dependent metabolic change has not been documented in bacterial systems.

Transcriptomic changes elicited by $H_2O_2$ have been profiled by previous microarray analyses in these two pathogenic bacteria. In *S. aureus*, genes associated with DNA repair, virulence, and iron uptake and storage are upregulated by oxidative stress. Notably, genes related to anaerobic metabolism and cytochrome *d* oxidase genes are induced at 20 min after treatment with $H_2O_2$ (26). In *P. aeruginosa*, DNA repair proteins, catalases, intracellular iron transport, and regulation are important for bacterial adaption to oxidative stress. Hydrogen peroxide induced the expression of all F-, R-, and S-type pyocins, leading to self-killing activity via DNA breakage and lipid biosynthesis inhibition (27).

We recently found that both bacteria can rapidly degrade $H_2O_2$ in several minutes, which leads to the question of whether the *in vitro* one-dose treatment with $H_2O_2$ would induce the comprehensive responses that are elicited by host-derived steady-state levels of $H_2O_2$ *in vivo* (16). As expected, our transcriptome sequencing (RNA-seq) analyses using a steady level of $H_2O_2$ stress uncovered significantly more genes that belong to pathways, such as those involved in glycolysis, virulence, translation, and RNA metabolism. The subsequent assays demonstrated that upon ROS stress, the elevated levels of fructose 1,6-biphosphate (FBP) and 2-keto-3-deoxy-6-phosphogluconate (KDPG) lead to dissociation of their corresponding glycolytic repressors from their cognate promoters, thus causing derepression of glycolytic genes to overcome $H_2O_2$-stalled glycolysis.

## MATERIALS AND METHODS

**Strains, plasmids, and primers.** Strains, plasmids, and primers are listed in Table S1 in the supplemental material. The *Pseudomonas aeruginosa* MPAO1 strain was maintained in LB medium. The *Staphylococcus aureus* Newman strain was cultured in Trypticase soy broth (TSB) medium. For plasmid maintenance in *P. aeruginosa* and *Escherichia coli*, the medium was supplemented with 50 μg/ml carbenicillin and 100 μg/ml ampicillin, respectively.

**Metabolite preparation and quantification using LC-MS.** For isolation of water-soluble metabolites, an ethanol-water protocol was used as previously described (28). Briefly, wild-type (WT) *P. aeruginosa* MPAO1 or *S. aureus* Newman strains were grown aerobically in LB or TSB medium for overnight at 37°C, diluted 100-fold in 20 ml of fresh medium, and incubated at 37°C with shaking at 250 rpm for 3 h (optical density at 600 nm [$OD_{600}$] of ~0.6). To examine the effect of oxidative stress on the metabolites, 20 ml of mid-log-phase cultures was placed in a dialysis bag (10 kDa) with shaking in 1 liter of LB or TSB containing 10 mM $H_2O_2$ for 10 min. The control sample was also dialyzed against medium without $H_2O_2$ for 10 min. Bacteria were collected by centrifugation for 5 min at 5,000 × *g* at 4°C and then washed once by prechilled 0.6% NaCl solution at 4°C. One milliliter of prechilled 60% ethanol solution was used to resuspend the pellet, which was then snap-frozen in liquid nitrogen. The bacterial pellets were subjected to two rounds of bead disruption (Fast Prep EP120 instrument; Qbiogene) at 4°C. After centrifugation, the supernatant was stored at −80°C or injected directly into the mass spectrometer. Detailed liquid chromatography-mass spectrometry (LC-MS) procedures have been described previously (29). Four biological repeats were included for each sample.

**RNA-seq, data analyses, and qRT-PCR verifications.** To examine the effect of oxidative stress on the transcriptome, 10 ml of mid-log-phase bacterial cultures (*P. aeruginosa* and *S. aureus*) were placed in a dialysis bag (10 kDa) with shaking in 1 liter of LB or TSB containing 10 mM $H_2O_2$ for 10 min. The control sample was also dialyzed against medium without $H_2O_2$ for 10 min. An RNeasy minikit (Qiagen) was used for subsequent RNA purification with DNase I treatment. After removing rRNA by using the MICROBExpress kit (Ambion), mRNA was used to generate the cDNA library according to the TruSeq RNA sample prep kit protocol (Illumina), which was then sequenced using the HiSeq 2000 system (Illumina). Bacterial RNA-seq reads were mapped to the *P. auruginosa* and *S. aureus* genomes by using TopHat (version 2.0.0), with two mismatches allowed (30). Only the uniquely mapped reads were kept for the subsequent analyses. The gene differential expression analysis was performed using Cuffdiff software (version 2.0.0) (31). Quantitative reverse transcription-PCR (qRT-PCR) was performed to verify the transcriptional changes for several glycolytic genes (*gapA*, *gapR*, and *fbp* of *S. aureus*, as well as *gapA*, *zwf*, *filC*, *filD*, *flgE*, *algU*, *algG*, and *mucA* from *P. aeruginosa* [primers shown in Table S4 in the supplemental material]). GO enrichment analyses were conducted on all differentially transcribed genes using DAVID (32) before data sets were imported into Cytoscape with an Enrichment Map plugin (33).

**Statistical analysis.** RNA-seq analyses were repeated twice. All other experiments were repeated at least three times. Two-tailed Student's *t* tests were performed using Microsoft Office Excel 2011.

**MIC measurements.** MICs of $H_2O_2$ were measured by using a microdilution technique according to NCCLS guidelines (34) in Mueller-Hinton broth. TSB medium was used to grow *S. aureus* in a 96-well plate. The MIC value was recorded as the lowest concentration at which there was no visible growth of *S. aureus*.

**Protein purification for GapR, HexR, and Eda.** For the expression of GapR, HexR, and Eda, we used the ligation-independent cloning (35) method (36). The respective coding regions were PCR amplified from either *S. aureus* (GapR) or *P. aeruginosa* (HexR and Eda) genomic DNA with the primers listed in Table S1 in the supplemental material (GapR-EXF/R for GapR, HexR-EXF/R for HexR, and Eda-EXF/R for Eda). The PCR products were treated with T4 DNA polymerase in the presence of dCTP for 30 min at room temperature. Target vector pMCSG19 (36) was digested with SspI, gel purified, and then treated with T4 DNA polymerase in the presence of dGTP for 15 min at 16°C. The T4 DNA polymerase-treated plasmid vector and PCR product were gel purified, mixed, incubated for 5 min at room temperature, and then transformed into *E. coli* strain DH5. The resulting plasmid was transformed again into BL21 Star(DE3) containing a plasmid (pRK1037) expressing tobacco vein mottling virus (TVMV) protease (Science Reagents, Inc.), and the transformants were selected on LB agar plates with 100 μg/ml ampicillin and 50 μg/ml kanamycin. The BL21 Star(DE3) strain carrying the plasmid was grown in LB to an optical density at 600 nm ($OD_{600}$) of 0.6, and then 1 mM isopropyl-β-D-thiogalactopyranoside (IPTG) was added. After overnight induction at 16°C, the cells were harvested and frozen at −80°C. The expressed protein was purified from the frozen cells with a HisTrap column (GE Healthcare, Inc.) by following the column manufacturer's recommendations. The purified protein was supplemented with 20% glycerol and stored at −80°C.

**EMSA.** The electrophoretic mobility shift assay (EMSA) was performed as follows. DNA probes containing promoter regions of *gapR* (*S. aureus*), *zwf* (*P. aeruginosa*), and *gapA* (*P. aeruginosa*) were PCR amplified using primers gapR-GSF/R, zwf-GSF/R, and gapA-GSF/R, respectively (listed in Table S1 in the supplemental material). The PCR products were radiolabeled with T4 polynucleotide kinase (NEB) and [$\gamma$-$^{32}$P]ATP (Perkin-Elmer). The radioactive probe (2 ng) was mixed with various amounts of the GapR or HexR protein in 20 μl of gel shift loading buffer (10 mM Tris-HCl, pH 7.4, 50 mM KCl, 5 mM $MgCl_2$, 10% glycerol, 3 μg/ml sheared salmon sperm DNA). After being incubated at room temperature for 20 min, the samples were analyzed by 8% (for *S. aureus gapR*)

or 6% (for *P. aeruginosa zwf* or *gapA*) polyacrylamide gel electrophoresis (100 V for prerun and 85 V for 45 min for sample separation). The gels were dried and subjected to autoradiography on a phosphor screen (BAS-IP; Fuji). The assay was repeated at least for three times with similar results.

**Dye primer-based DNase I footprint assay.** The DNase I footprint procedures were modified according to reference 37. The promoter regions from *gapR* or *zwf* were generated by PCR with the primers gapR-FP-6FAM and gapR-GSR as well as zwf-FP-6FAM and zwf-GSR (see Table S1 in the supplemental material). About 50 ng of 6-carboxyfluorescein (6-FAM)-labeled *gapR* or *zwf* promoters was incubated with 1 μM GapR or HexR protein in a binding buffer (10 mM Tris-HCl [pH 7.4], 50 mM KCl, 5 mM $MgCl_2$, 10% glycerol, 3 μg/ml sheared salmon sperm DNA). Kunitz DNase I (0.05 units) (New England BioLabs) was used to incompletely digest promoter DNA in the reaction mixture for 5 min at room temperature. The reaction was stopped with 0.25 M EDTA and extracted with phenol-chloroform-isoamyl alcohol (25:24:1). The DNA fragments were purified with the QIAquick PCR purification kit (Qiagen) and eluted in 15 μl distilled water. About 5 μl of digested DNA was added to 4.9 μl HiDi formamide (Applied Biosystems) and 0.1 μl GeneScan-500 LIZ size standards (Applied Biosystems). The samples were analyzed with the 3730 DNA analyzer, with the G5 dye set, running an altered default genotyping module that increased the injection time to 30 s and the injection voltage to 3 kV at the sequencing facility at the University of Chicago. Results were analyzed with Peak Scanner (Applied Biosystems). The assay was repeated at least three times with similar results.

**Persister killing assay.** Procedures followed previously published protocols (38). For the preparation of *S. aureus* persisters, bacterial cells were shaken at 37°C in TSB medium to an $OD_{600}$ of 0.3. Cells were then diluted 1:1,000 in 25 ml fresh TSB medium and grown for 16 h at 37°C. Cultures were then treated for 4 h with 5 μg/ml ofloxacin under the growth conditions stated above. Persisters were then washed with 10 ml of filtered phosphate-buffered saline (PBS) and resuspended in M9 minimal medium. Glucose (1 mM) and kanamycin (30 μg/ml) were added, and samples were incubated at 37°C. After 2 h, samples were washed twice with PBS to remove excessive antibiotics. Ten-microliter aliquots of samples were removed, serially diluted, and spot plated onto TSB agar plates to determine CFU/ml. The survival percentage was determined by dividing the CFU/ml of a sample at each time point by the initial CFU/ml for that sample.

**FBP assay.** FBP was quantified enzymatically by a coupled assay, adapted from the assay described previously (39, 40), which was carried out in an imidazole buffer (150 mM [pH 7.4]) containing 9 mM MgSO4 by measuring the consumption of NADH (absorbance at 340 nm) by glycerol-3-phosphate dehydrogenase. Ten microliters of metabolic extraction (from the metabolite quantification) was added to a 90-μl reaction mixture containing 0.23 mM NADH, aldolase (0.15 U/ml [Sigma]) triosephosphate isomerase (2 U/ml [Sigma]), and glycerol-3-phosphate dehydrogenase (0.2 U/ml [Sigma]) in imidazole buffer. After 5 min at room temperature, the $OD_{340}$ was recorded. Pure FBP (Sigma) standards were used to prepare a standard curve. Finally, the intracellular FBP concentrations were calculated by estimating bacterial intracellular volume as 1.5 μl/mg bacterial dry weight (41).

**KDPG assay.** Intracellular KDPG concentrations were measured enzymatically with coupling of KDPG aldolase (Eda, purified recombinant protein) to lactate dehydrogenase (LDH) (Sigma), which is modified from the method used by Cheriyan and colleagues (42). KDPG is catalyzed to pyruvate, which is then measured by the decrease in NADH absorbance at 340 nm in 100 μl of reaction solution containing HEPES (100 mM [pH 7.5]), NADH (250 μM), LDH (0.023 U/ml), and 1 μM Eda. Pure KDPG (Sigma) standards were used to prepare a standard curve. The intracellular KDPG concentrations were calculated by estimating bacterial intracellular volume as 1.5 μl/mg bacterial dry weight (41).

**Glucose uptake assay and growth assay for *P. aeruginosa*.** *P. aeruginosa* MPAO1 was grown in LB until it reached an $OD_{600}$ of 0.6 before being transferred to new LB medium containing 3% D-glucose. In the presence or absence of 400 μM iodoacetic acid (IAA), *P. aeruginosa* was then cultured for 2 h before the remaining glucose concentrations were determined by the QuantiChrom glucose assay kit (Bioassay systems). The growth rate was measured by $OD_{600}$.

**Construction of a clean deletion *P. aeruginosa* strain (gene PA3001, which encodes GAPDH).** The ΔPA3001 strain was constructed by a strategy using the suicide vector pEX18Ap (43). Briefly, the 2-kb fragments of the upstream region of the PA3001 gene were amplified using primers PA3001DupF (with a HindIII site) and PA3001DUpR (with an XbaI site) (see Table S1 in the supplemental material). The primers PA3001DDnF (with an XbaI site) and PA3001DDnR (with an EcoRI site) were used for amplification of 2 kb of PA3001 downstream region. The two respective PCR products were digested with HindIII-XbaI or XbaI-EcoRI, respectively, and then cloned into HindIII/EcoRI-digested gene replacement vector pEX18Ap via a three-piece ligation, yielding pEX18Ap-PA3001UD. A 0.8-kb gentamicin resistance cassette was cut from pPS858 with XbaI and then cloned into pEX18Ap-PA3001UD, yielding pEX18Ap-PA3001UGD. The resultant plasmid was electroporated into MPAO1 with selection for gentamicin resistance. Colonies were screened for gentamicin sensitivity and loss of sucrose (5%) sensitivity, which typically indicates a double-crossover event and is indicative of gene replacement. The resulting ΔPA3001 strain was further confirmed by PCR analysis.

**NADPH assay.** The intracellular concentration of NADPH was measured using the EnzyChrom $NADP^+$/NADPH assay kit from BioAssay Systems. Bacteria of the wild-type *P. aeruginosa* MPAO1 or *S. aureus* Newman strain were grown in LB or TSB medium overnight at 37°C, diluted 100-fold in 20 ml of fresh medium, and incubated at 37°C with shaking at 250 rpm for 3 h ($OD_{600}$ of ~0.6). To examine the effect of oxidative stress on NADPH, 20 ml of mid-log-phase culture was placed in a dialysis bag (10 kDa) with shaking in 1 liter of LB or TSB containing 10 mM $H_2O_2$ for 10 min. Bacteria were collected by centrifugation for 5 min at 5,000 × *g* at 4°C and then were washed once with prechilled 0.6% NaCl solution at 4°C before following the manufacturer's instructions.

**$H_2O_2$ assay.** The concentrations of $H_2O_2$ inside the dialysis bag during the 10-min dialysis (starting with 10 mM $H_2O_2$) were measured using the Amplex Red hydrogen peroxide/peroxidase assay kit (Life Technologies). The medium was taken from the dialysis bag at certain time points before following the manufacturer's instructions.

**Microarray data accession number.** The RNA-Seq data files have been deposited in NCBI's Gene Expression Omnibus (GEO) and can be accessed through GEO series accession no. GSE55528.

## RESULTS

**Steady-state levels, but not one-dose treatments with $H_2O_2$, induce PPP following inhibition of GAPDH.** Like many other organisms, GAPDH from both *P. aeruginosa* and *S. aureus* can be readily inhibited by ROS-mediated direct oxidation of their catalytically active cysteines (16). We speculated that inhibition of GAPDH leads to an elevated pentose phosphate pathway (PPP), which has been observed in yeast (*Saccharomyces cerevisiae*) (25). This hypothesis also implies that bacteria generate more NADPH to protect from ROS; NADPH is the main cellular reducing agent used by bacterial protective enzymes in reducing $H_2O_2$ and related oxidants (44). In order to verify this speculation, we cultured *P. aeruginosa* and *S. aureus* until mid-log phase and treated the bacteria with one dose of $H_2O_2$ (10 mM) for 20 min as commonly used previously. After extracting intracellular metabolites from the bacteria, we utilized LC-tandem MS (LC-MS/MS) to quantify the intracellular concentrations of a group of glycolytic and PPP metabolites in $H_2O_2$-treated versus untreated controls. There were no significant changes observed in metabolite levels post-$H_2O_2$ treatment (see Fig. S1A in the supplemental material).

Given that both bacteria are able to completely degrade 10 mM $H_2O_2$ within minutes (16), we changed our approach and continuously treated bacteria (10 ml of mid-log-phase culture) with 1 liter medium containing 10 mM $H_2O_2$ for 10 min in a dialysis bag (10-kDa cutoff). We measured the actual $H_2O_2$ concentrations inside the dialysis bag at different time points (0, 1, 2, 5, and 10 min) during the 10-min dialysis. As shown in Fig. S1B in the supplemental material, the concentration ranges from 3 to 7 mM, indicating the steady state of $H_2O_2$ exposed to bacteria via this method. Under the new conditions, the levels of glucose-6-phosphate/fructose-6-phosphate (G6P/F6P), glucose or fructose biphosphate (G2P/F2P), and ribose-5-phosphate (R5P) were significantly increased after $H_2O_2$ exposure in both pathogens (Fig. 1A), indicating that the inactivation of GAPDH likely elevates PPP metabolites. Finally, we also detected a higher concentration of the reduced glutathione (GSH) in the $H_2O_2$-treated *P. aeruginosa*, which strongly suggests that the increased NADPH is used to generate more GSH (via glutathione reductase) to counter oxidative stress in *P. aeruginosa* (Fig. 1A). The different effects between one-dose and steady-dose $H_2O_2$ led us to test if one-dose $H_2O_2$ would also elicit a similar metabolic change at early time points. As expected, we were able to observe induced levels of glycolytic and PPP metabolites at 2 min but not after 10 min after one dose of 10 mM $H_2O_2$ (see Fig. S1C).

If the metabolic change is dependent on GAPDH, its mutant would display a similar metabolic change as elicited by the steady dose of hydrogen peroxide supplement. There are two GAPDH enzymes in *S. aureus*, GapA and GapB, which are predicted to catalyze the glycolytic oxidation of GAP and the reverse gluconeogenic reaction, respectively (22). In order to verify this hypothesis, we obtained an *S. aureus gapA* (SAOUHSC_00795 [encodes GAPDH]) deletion mutant from J. A. Morrissey at the University of Leicester, and constructed a *P. aeruginosa* PA3001 (encodes GAPDH) deletion mutant by exchanging a gentamicin resistance gene with the PA3001 gene in the chromosome. Intracellular metabolites were extracted from these mutants and their parent wild-type (WT) strains and quantified by LC-MS. As shown in Fig. S1E in the supplemental material, these mutants indeed displayed a decrease in NADH and elevated levels of PPP metabolites. Different from the WT, these mutants displayed no significant metabolic changes in the absence or presence of a steady dose of $H_2O_2$ treatment (see Fig. S1F), which further confirms the essential role of GAPDH in hydrogen peroxide-induced metabolic change.

We next tested if inactivation of GAPDH could result in an increased anti-ROS response in bacteria. The mutation in *gapA* affected growth and therefore was not used (data not shown). We then supplemented the culture medium with iodoacetic acid (IAA [400 μM]), which is a known inhibitor of GAPDH (45), and then measured the MIC to $H_2O_2$ of IAA-treated and untreated bacteria. As shown in Fig. 1B, IAA-treated *S. aureus* displayed a 4-fold higher MIC to $H_2O_2$ than the untreated control, indicating that the GAPDH blockage indeed enables bacterial resistance to ROS. Our metabolic quantification and subsequent MIC measurements indicate that oxidative inactivation of GAPDH functions as a metabolic switch that maintains NADPH/$NADP^+$ equilibrium during oxidative stress in bacterial pathogens.

Recently, a combination of specific glycolytic metabolites (glucose, mannitol, fructose, or pyruvate) and aminoglycosides have been presented as the first strategy capable of eradicating bacterial persisters, a notorious subpopulation of dormant bacteria that can tolerate antibiotic treatment (38). Catabolism of these metabolites generates NADH via glycolysis. After being oxidized by the electron transport chain, NADH contributes to proton motive force (PMF) that promotes aminoglycoside uptake and the killing of persisters. This observation points to the importance of the bacterial metabolites in antibiotic mechanism of action. Integrating these results with $H_2O_2$-mediated inhibition of GAPDH led us to speculate that ROS inactivation of GAPDH could decrease NADH and PMF, thus disabling persister eradication. To test this hypothesis, we cultured *S. aureus* until the mid-log phase and treated bacteria with 1 mM $H_2O_2$ (in a dialysis bag) or 400 μM IAA for 1 h. After extracting intracellular metabolites from the bacteria, we utilized LC-MS/MS to quantify the intracellular concentration of NADH and compared it to that of the untreated controls. The NADH level in *S. aureus* was significantly decreased after exposure to $H_2O_2$ or IAA (Fig. 1C). We measured the *S. aureus* persister killing by both glucose and kanamycin in the presence of 1 mM $H_2O_2$ or 400 μM IAA. As shown in Fig. 1D, a 100-fold increase of persister survival was observed in the presence of 1 mM $H_2O_2$ or 400 μM IAA compared to the untreated control. In the absence of $H_2O_2$, the persisters derived from the *gapA* deletion displayed higher resistance to kanamycin than those from the WT (Fig. 1D). Taken together, our results showed that the activity of GAPDH plays an important role in the metabolite-based persister eradication (Fig. 1E).

**RNA-seq analyses revealed that steady-state levels of $H_2O_2$ elicited profound transcriptional changes, including induced glycolysis in pathogenic bacteria.** It is estimated that a steady-state level of superoxide is produced by NADPH oxidase in a phagosome (1, 46). The observation of induced glycolysis under only steady levels of ROS stress strongly suggests that a steady-state stress of $H_2O_2$ might induce broader and greater transcriptional fluctuation than the one-dose $H_2O_2$ that had been used in previous microarray analyses (26, 47). With this in mind, we decided to employ RNA-seq to examine the transcriptomes of *S. aureus* Newman and *P. aeruginosa* MPAO1 in response to continuous treatment with 10 mM $H_2O_2$ (in a dialysis bag for 10 min), a concentration commonly used by other studies since both pathogens can tolerate millimolar levels of $H_2O_2$ well (26, 48, 49). The same practice with a dialysis bag has been used in previous studies to expose bacteria to a steady-state level of $H_2O_2$ (48, 50). We measured bacterial numbers of both pathogens in the presence and absence of a steady dose of 10 mM $H_2O_2$ for 10 min with no difference observed (see Fig. S1D in the supplemental material). Therefore, we added sufficient but not deleterious $H_2O_2$ in order to ensure that most steady $H_2O_2$-responsive changes could be revealed in our transcriptomic experiments. Using replicate experiments, we identified a total of 458 *S. aureus* genes (17.1% of the genome; 208 upregulated and 250 downregulated) and 1,722 *P. aeruginosa* genes (31.2% of the genome; 1,113 upregulated and 709 downregulated), whose mRNA levels were altered in response to a steady-state treatment with $H_2O_2$, compared to the control without $H_2O_2$ treatment (Fig. 2A; see Tables S2 and S3 in the supplemental material). As expected, these numbers were significantly greater than those in previous microarray analyses based on one-dose $H_2O_2$ treatment (12.7% of the *S. aureus* genome and 9.3% of the *P. aeruginosa* genome), suggesting profound global transcriptional changes with steady-state stress of $H_2O_2$. Our new finding represents transcripts of genes that may be activated or

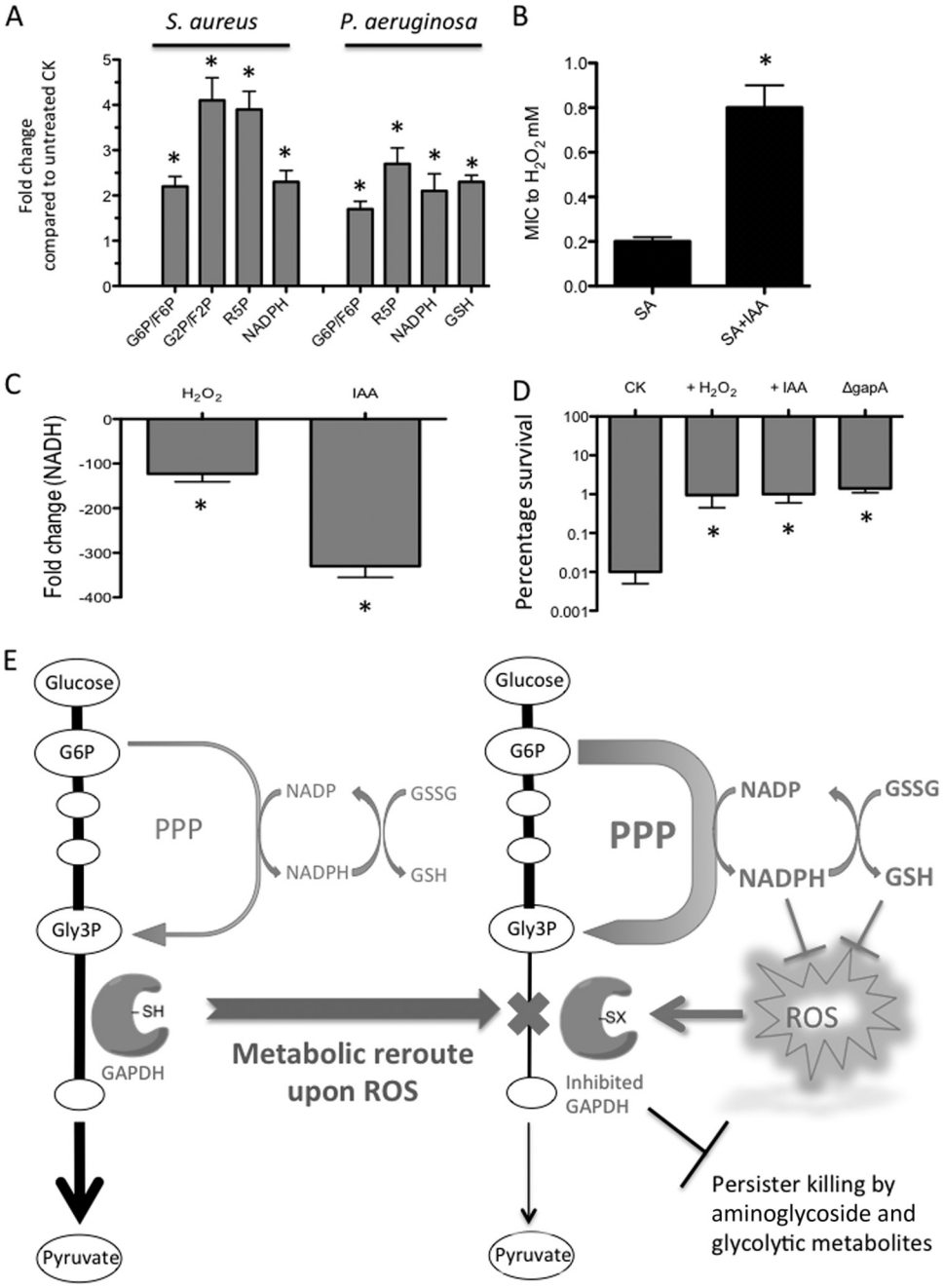


**FIG 1** Steady-state treatment with $H_2O_2$ induces PPP following inhibition of GAPDH. (A) Changes in metabolite levels in *P. aeruginosa* or *S. aureus* treated with and without a steady dose of 10 mM $H_2O_2$ for 10 min. Bacterial lysates were prepared, and metabolites were quantified by LC-MS/MS. The absolute metabolite concentrations were normalized and are presented as fold changes compared to the untreated control (CK). The asterisks denote that the differences between $H_2O_2$-treated and untreated samples are statistically significant ($P < 0.05$). (B) MIC of $H_2O_2$ for *S. aureus* RN4220 strains in Mueller-Hinton broth. SA, wild-type strain RN4220; SA + IAA, wild-type RN4220 supplemented with 400 μM iodoacetic acid. The asterisks denote that the differences from the untreated wild type are statistically significant ($P < 0.05$). (C) Changes in intracellular NADH levels in *S. aureus* treated with and without 1 mM $H_2O_2$ or 400 μM IAA for 10 min. Bacterial lysates were prepared, and metabolites were quantified by LC-MS/MS. The absolute metabolite concentrations were normalized and are presented as changes in percentage compared to the untreated control. The asterisks denote that the differences between $H_2O_2$-treated and untreated samples are statistically significant ($P < 0.05$). (D) Percentage of survival of *S. aureus* persisters after treatment with 30 μg/ml kanamycin and 1 mM glucose. Addition of 1 mM $H_2O_2$ or 400 μM IAA promoted survival of the persisters. Persisters derived from the *gapA* deletion are around 150-fold more resistant to kanamycin than the WT. The asterisk denotes that the difference is statistically significant ($P < 0.05$). (E) ROS inactivation of GAPDH leads to a metabolic reconfiguration from glycolysis to the pentose phosphate pathway, thus increasing the intracellular levels of NADPH and GSH that are involved in counteracting oxidative stress. ROS-induced inhibition of GAPDH leads to the reduced production of NADH and PMF, thus repressing the eradication of metabolite-based persisters.

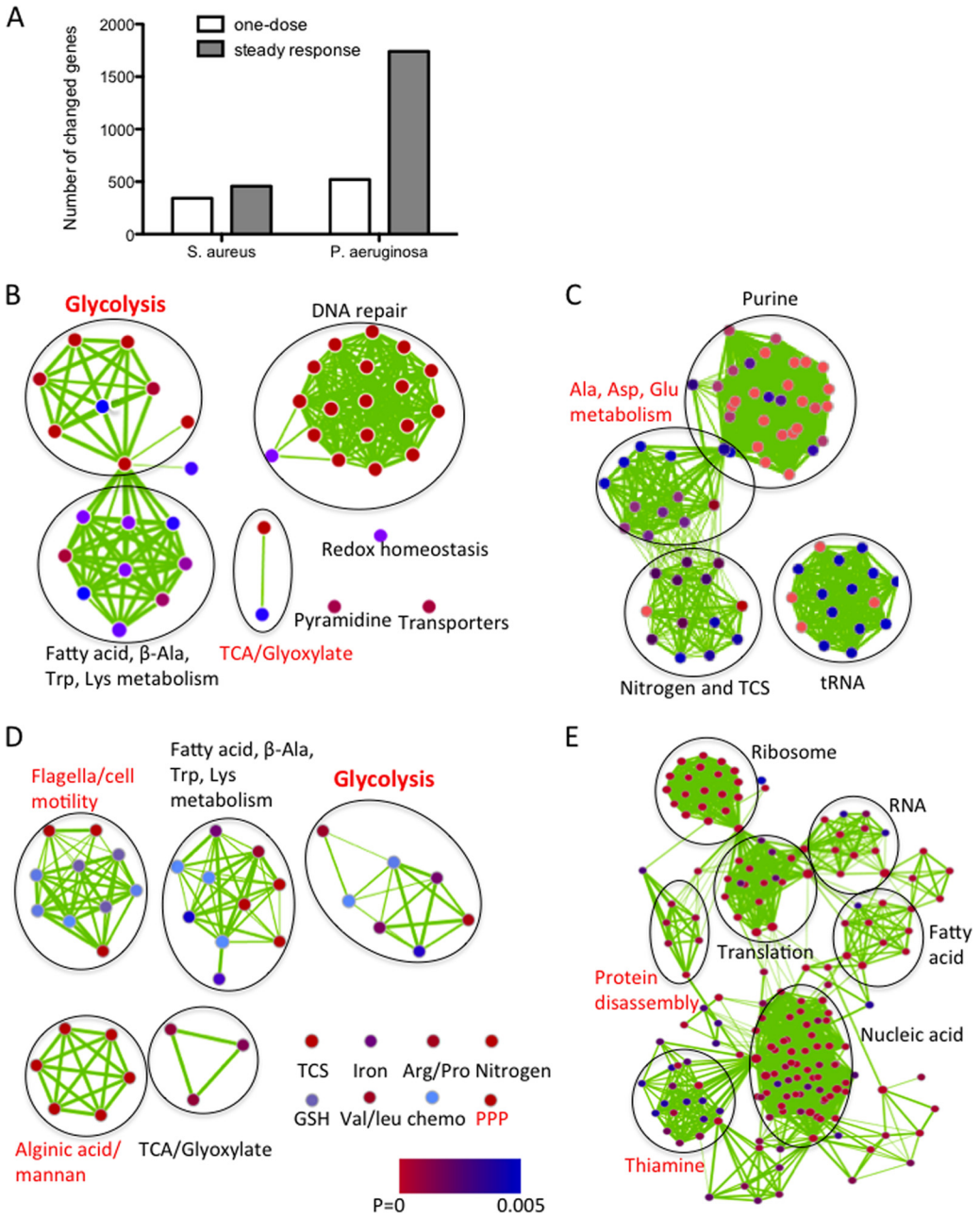


**FIG 2** Steady-state $H_2O_2$ stress can elicit profound transcriptional changes in bacteria. (A) Comparison of numbers of changed genes between previous microarray analyses based on one-dose treatment with $H_2O_2$ and the current RNA-seq analyses using steady-state treatment with $H_2O_2$. (B and C) GO enrichment analysis of all genes in *S. aureus* upregulated or downregulated, respectively, by a steady dose of $H_2O_2$. (D and E) GO enrichment analysis of all genes in *P. aeruginosa* upregulated or downregulated, respectively, by a steady dose of $H_2O_2$. Pathways that are not reported in previous microarray analyses are highlighted in red. All *P* values of the nodes are $<0.005$.

repressed during interaction with host macrophages that consistently produce a steady dose of peroxide (1).

Based on SP-PIR (Protein Information Resource) keyword designations, these differentially expressed genes were classified into multiple functional categories, including many metabolic pathways and stress responses (see Fig. S2A and S2B, respectively, in the supplemental material for *S. aureus*, as well as Fig. S2C and S2D, respectively, for *P. aeruginosa*). In *S. aureus*, Gene Ontology (GO) enrichment analysis showed significant enrichment for genes related to glycolysis, the tricarboxylic acid (TCA) cycle, DNA repair, redox homeostasis, transporters, pyrimidine, and fatty acid and amino acid (β-Ala, Trp, and Lys) biosynthesis among the genes upregulated by the steady-state treatment with $H_2O_2$ ($P < 0.005$) and purine, tRNA, nitrogen, two-component systems, and amino acid (Ala, Asp, and Glu) metabolism among downregulated genes ($P < 0.005$) (Fig. 2B and C). Among these categories, genes involved in glycolysis, the TCA cycle, and several amino acid biosynthesis pathways were not identified in previous

one-dose-based microarray analyses (highlighted in red in Fig. 2B and C), indicating that these pathways are affected in response to a steady level of $H_2O_2$.

The GO enrichment analysis of all changed genes in *P. aeruginosa* generated more pathways with complicated patterns (Fig. 2D and E). Notably, in the presence of a steady-state level of $H_2O_2$, expression of genes coding for proteins involved in glycolysis, the pentose phosphate pathway, flagella, and alginic acid was induced, whereas expression of genes involved in translation, protein disassembly, and thiamine was repressed. Many of these genes were not responsive to one-dose treatment with $H_2O_2$ (highlighted in red in Fig. 2D and E). RT-PCR was performed for genes that are involved in flagellum and alginate pathways. As shown in Fig. S2E in the supplemental material, all tested genes (*filC*, *filD*, *flgE*, *algU*, *algG*, and *mucA*) were induced 1.5- to 2-fold by a steady-state level of $H_2O_2$ for 10 min. However, these expression changes did not translate into a phenotypic level (by either the swinging or biofilm test [data not shown]). We also took advantage of a recent annotation of *P. aeruginosa* small RNAs (sRNAs) to identify 18 sRNAs that were differentially transcribed under the steady-state stress of $H_2O_2$, such as transfer-messenger RNA (tmRNA), *rnpB*, and *crcZ* (51) (see Table S4 in the supplemental material).

**Steady-state $H_2O_2$ treatment leads to derepression of glycolytic genes through GapR in *S. aureus*.** Among the pathways that were highlighted in the GO enrichment analysis, genes encoding glycolytic enzymes were induced in both tested bacterial strains by steady-state levels of $H_2O_2$, suggesting that a common underlying mechanism is involved. In *S. aureus*, a total of seven genes associated with glycolysis (*gapR*, *gapA*, *pgk*, *tpiA*, *pgm*, *fbp*, and *pgi*) or PPP (*zwf*) are significantly upregulated by a steady-state treatment with $H_2O_2$ (2- to 4-fold) (Fig. 3A). First, to assess the reliability of RNA-seq data in representing the relative levels of individual transcripts, the identical RNA samples were subjected to real-time quantitative reverse transcription-PCR (qRT-PCR) in order to verify the mRNA levels of two glycolytic genes (*gapR* and *gapA*) and one gluconeogenic gene (*fbp*) with both control and steady-state treatments with $H_2O_2$. The qRT-PCR results matched with the corresponding RNA-seq data, ensuring its reliability in determining the transcriptional changes (Fig. 3B). We next aimed to test if the upregulated glycolytic genes would eventually lead to elevated levels of glycolytic metabolites. We utilized LC-MS/MS to quantify the intracellular concentrations of a group of glycolytic, PPP, and TCA metabolites in steady-state $H_2O_2$-treated versus untreated controls. The levels of phosphoenolpyruvate (PEP), glyceraldehyde-3-phosphate (GAP), 3-phosphoglycerate/2-phosphoglycerate (3PG/2PG), succinate, and citrate were significantly increased after $H_2O_2$ exposure in *S. aureus* (Fig. 3C), indicating that the steady-state challenge with $H_2O_2$ not only induces glycolytic genes but also elevates glycolytic and early TCA cycle metabolites.

As aforementioned, we showed that steady-state levels of $H_2O_2$ can cause an induction of both glycolysis and the pentose phosphate pathway, following inhibition of GAPDH. In light of this, the new observation of induced glycolytic genes by the steady-state treatment with $H_2O_2$ suggests a potential correlation between these two events. We propose that metabolite-mediated transcriptional regulation is involved for the glycolytic genes in *S. aureus*. Although the regulatory mechanism of staphylococcal glycolytic genes is not well documented, *S. aureus* has a glycolytic operon that is highly homologous to the well-studied counterpart in *B. subtilis* (23). In *B. subtilis*, the glycolytic operon contains six genes, beginning with *cggR* encoding the glycolytic repressor CggR, which tunes the transcription of itself and all other genes in the operon (*gapA*, *pgk*, *tpiA*, *pgm*, and *eno*) (Fig. 3D). CggR directly binds to a CggR motif consisting of two direct repeats (CG GGACN$_6$TGTC-N$_4$CGGGACN$_6$TGTC) in its own promoter (23). It has also been demonstrated that fructose-1,6-biphosphate (FBP) specifically interacts with CggR and functions as its derepressor by reducing its DNA-binding activity. Like *cggR*, *gapR* in *S. aureus* has been shown to negatively regulate its own glycolytic operon (Fig. 3E) (22). In the present study, glucose or fructose biphosphate (G2P/F2P), including FBP, exhibited a 4-fold accumulation upon steady-state treatment with $H_2O_2$ (Fig. 1A), suggesting that elevated FBP directly binds to GapR and induces the dissociation of GapR from its target DNA. We used an enzyme-based assay (see Materials and Methods) to measure the intracellular concentrations of FBP in *S. aureus*, which are 2.5 $\pm$ 0.5 mM (without $H_2O_2$ treatment) and 10 $\pm$ 3 mM (with a steady-state level of $H_2O_2$). These concentrations are comparable to the published concentration in *E. coli* (15 mM) (52).

We expressed and purified a His$_6$-tagged full-length *S. aureus* GapR protein from *E. coli* grown in Luria broth. As expected, the electrophoretic mobility shift assay (EMSA) showed that GapR binds to its own promoter efficiently and specifically (Fig. 4A; see Fig. S3A in the supplemental material). The dissociation constant ($K_d$) of the interaction between GapR and its own promoter was around 0.2 μM (see Fig. S3A). Importantly, there is a noticeable change in the binding of GapR to its own promoter DNA in the presence of 2.5 mM or 10 mM FBP. The GapR-DNA complex is not sensitive to 10 mM $H_2O_2$ or the other inorganic phosphate (3PG) (Fig. 4A). In order to further confirm the binding site of GapR on its own promoter (also the promoter of the glycolytic operon), we performed a DNase I footprint assay by using dye primer sequencing on the Applied Biosystems 3730 DNA analyzer. We were able to uncover a specific GapR-protected region (−100 to −56 away from ATG) on the *gapR* promoter (Fig. 4C). Interestingly, a putative GapR box (GAGGTTN$_6$TGTCN$_5$CGGG ACN$_6$AGGC, from −94 to −58) was located in this protected region, which is very similar to the CggR motif (CGGGACN$_6$TG TCN$_4$CGGGACN$_6$TGTC) found in *B. subtilis*. The predicted putative GapR box is located downstream of the −35 and −10 consensus sequences (highlighted in blue in Fig. 4C), which is characteristic of negative regulation by bacterial transcription factors (53). Indeed, *gapA* has been shown to be overexpressed in a *gapR* mutant, proving the direct negative regulation (22).

FBP is also a coactivator for CcpA, the carbon catabolite protein in many Gram-positive bacteria (54). In order to test if CcpA is involved in the FBP-mediated induction of the *gap* operon, we repeated experiments using a *gapR* mutant (from J. A. Morrissey at University of Leicester). Our RT-PCR assay revealed no significant induction of *gapA* by the steady-state level of $H_2O_2$ in the *gapR* mutant (see Fig. S3B in the supplemental material), which indicates that *gapR* is responsible for the induction of the *gap* operon in the WT.

**Steady-state treatments with $H_2O_2$ can elevate the level of 2-keto-3-deoxy-6-phosphogluconate (KDPG), which interacts with HexR and derepresses glycolytic genes in *P. aeruginosa*.** Like *S. aureus*, a group of glycolytic genes in *P. aeruginosa* were induced with steady-state treatment with $H_2O_2$, such as *gapA*, *pgm*, *edd*, *pgk*, *zwf*, and *pgl*, which were verified by a subsequent

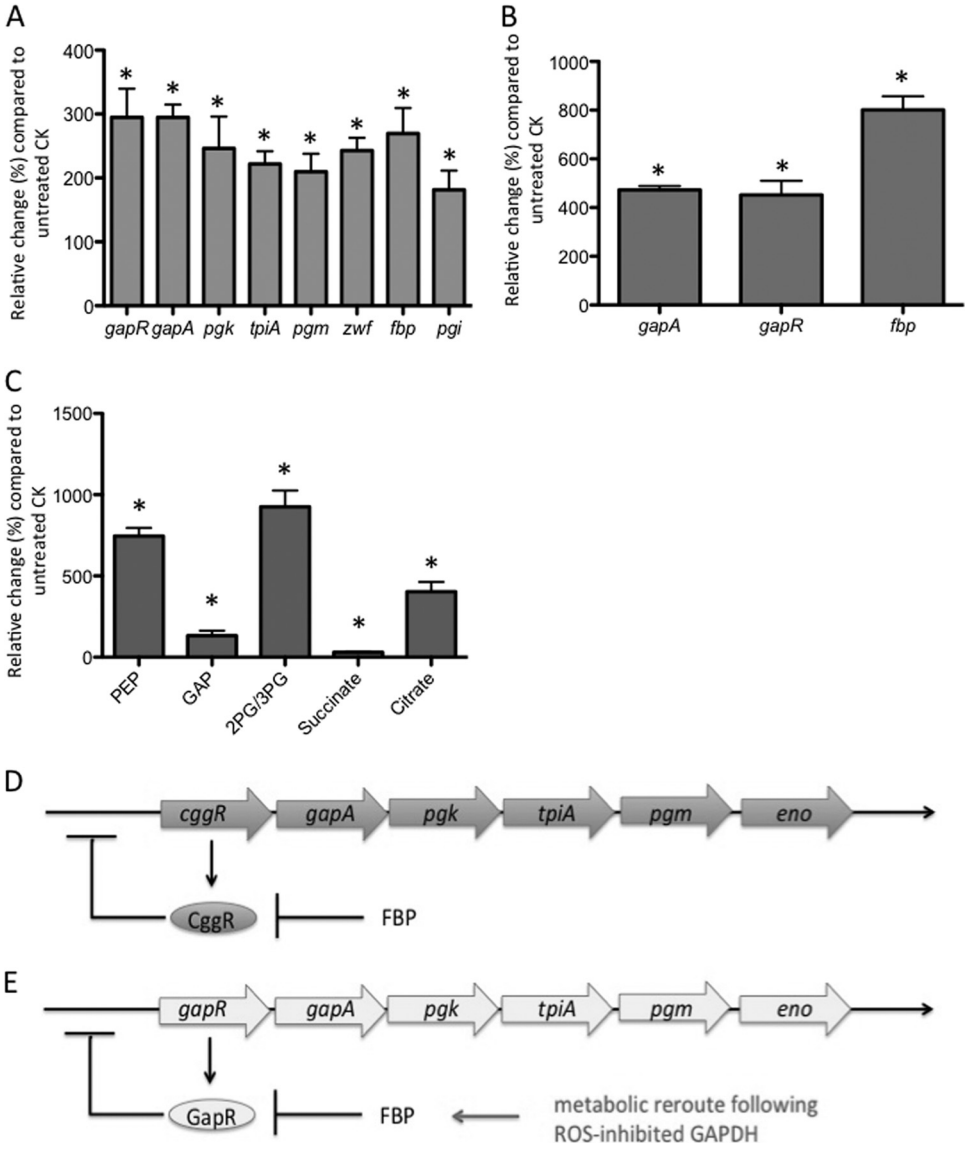


**FIG 3** Steady-state $H_2O_2$ treatment induces glycolysis in *S. aureus*. (A) Original RNA-seq results showed that a group of glycolytic genes were derepressed upon continuous treatment with $H_2O_2$ in *S. aureus*. (B) Quantitative real-time PCR (qRT-PCR) confirmed that the transcription levels of *S. aureus gapA*, *gapR*, and *fbp* were induced by treatment with a steady dose of $H_2O_2$. The asterisks denote that the differences between $H_2O_2$-treated and untreated samples are statistically significant ($P < 0.05$). (C) Changes in metabolite levels in *S. aureus* constitutively treated with and without 10 mM $H_2O_2$ for 10 min. Bacterial lysates were prepared, and metabolites were quantified by LC-MS/MS. The absolute metabolite concentrations were normalized and are presented as changes in percentage compared to the untreated control. (D and E) Gene organization in the glycolytic operon loci of *B. subtilis* and *S. aureus*, respectively. The interaction between CggR and FBP leads to the dissociation of the CggR-DNA complex, resulting in derepression of glycolytic genes. The asterisks denote that the differences between $H_2O_2$-treated and untreated samples are statistically significant ($P < 0.05$).

qRT-PCR assay (Fig. 5A and B). Our metabolomic analysis also demonstrated that the levels of glycolytic and early TCA metabolites, such as PEP, 3PG/2PG, 6PG/6PF, succinate, citrate, and ATP, were significantly increased after $H_2O_2$ exposure in *P. aeruginosa* (Fig. 5C).

In *Pseudomonas* species, glycolysis is linked with the Entner-Doudoroff (ED) pathway, which is extensively studied in *Pseudomonas putida* and contains two operons (*zwf-pgl-eda* and *edd-glk-gltR2-gltS*) (55). The transcription of these operons is controlled by the repressor HexR, which directly binds to an inverted repeat ($TTGTN_{7-8}ACAA$) in these two promoters, which is released by the specific binding of the ED pathway intermediate 2-keto-3-deoxy-6-phosphogluconate (KDPG) to HexR (24). The orthologs of these glycolysis ED genes are organized in a similar way in *P. aeruginosa*, which have not been well characterized (Fig. 5D). We propose that the steady-state levels of $H_2O_2$ elevate the intracellular level of KDPG, which subsequently binds to HexR en route to derepression of glycolysis ED genes. We measured the level of KDPG by employing a coupled assay combining KDPG edolase (EDA [cloned from *P. aeruginosa* and purified from *E. coli*]) and lactate dehydrogenase (LDH [Sigma]). The production of pyruvate from KDPG was measured by the decrease in NADH absorbance at 340 nm (42). As expected, the steady-state treatment with $H_2O_2$ significantly elevated the intracellular concentra-

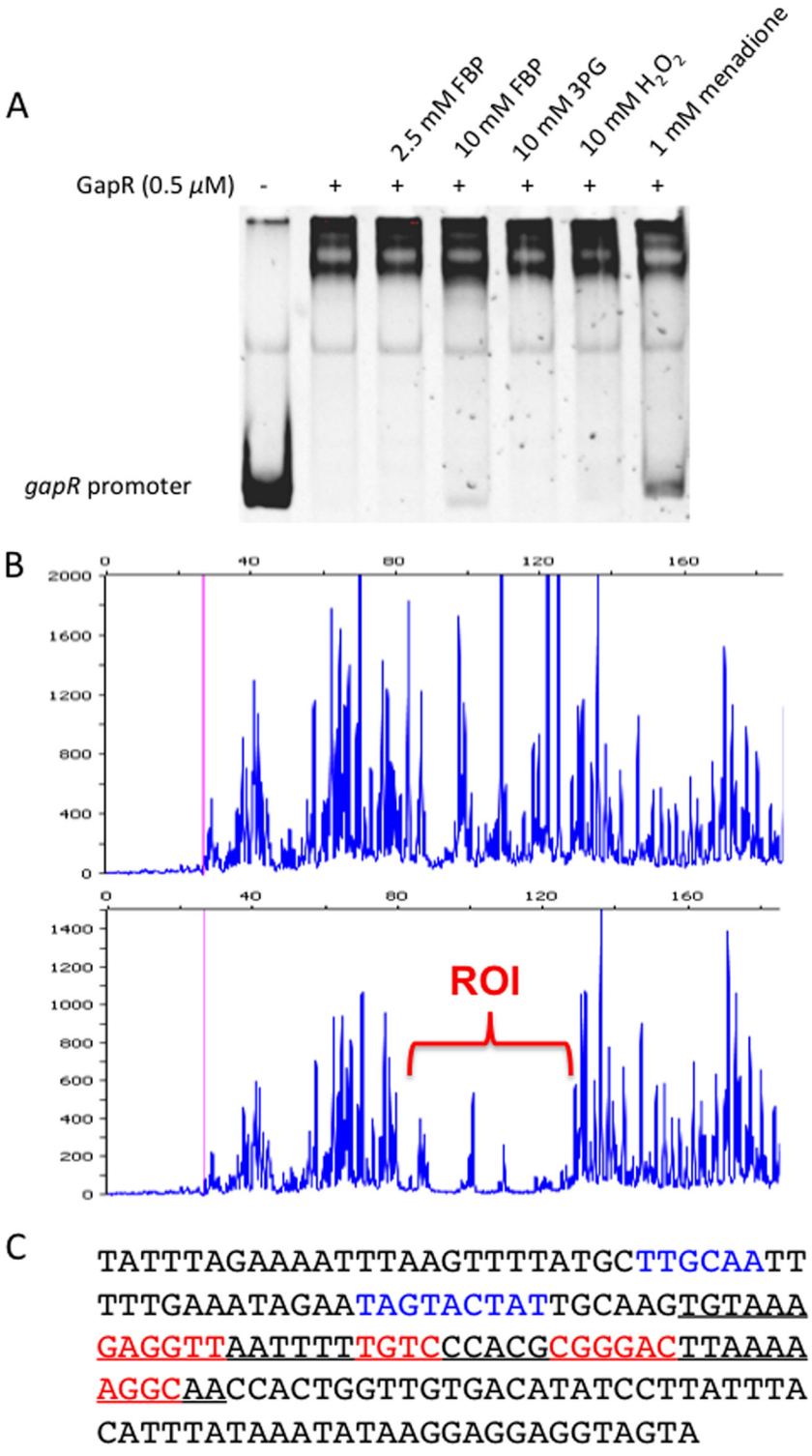


**FIG 4** Fructose 1,6-biphosphate (FBP) releases the repression of glycolytic genes through GapR in *S. aureus*. (A) EMSA shows that GapR directly binds to its own promoter. There is a noticeable dissociation of the GapR-DNA complex in the presence of 10 mM FBP (but not in the presence of 2.5 mM FBP), which is the calculated *in vivo* concentration after a steady dose of 10 mM $H_2O_2$. The GapR-DNA complex is not sensitive to either 10 mM $H_2O_2$ or 3PG but is sensitive to 1 mM menadione. (B) GapR directly binds to a CggR box-like motif in its own promoter according to a dye primer-based DNase I footprint assay. Electropherograms show the protection patterns of the *gapR* promoter after digestion with DNase I following incubation in the absence (upper panel) or presence (lower panel) of 1 μM GapR. ROI, region of interest. (C) *gapR* promoter sequence (−160 from ATG) with a summary of the DNase I footprint assay results. The −35 and −10 promoter regions are highlighted in blue. The GapR-protected region is underlined, and the two putative repeats in the GapR motif are highlighted in red.

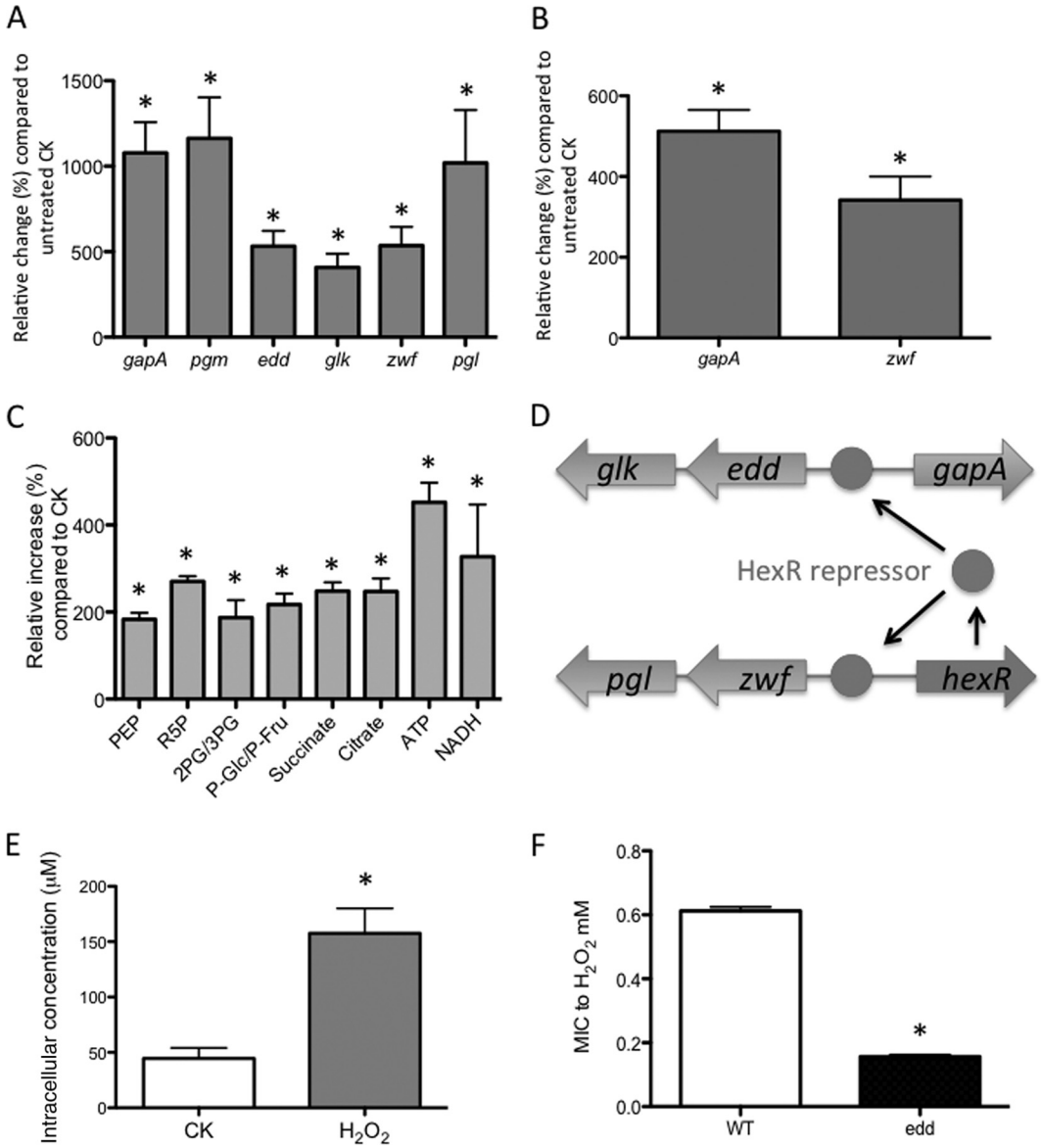


**FIG 5** Steady-state treatment with $H_2O_2$ induces glycolysis in *P. aeruginosa*. (A) The original RNA-seq results showed that a group of glycolytic genes were derepressed upon continuous treatment with $H_2O_2$ in *P. aeruginosa*. (B) Quantitative real-time PCR (qRT-PCR) confirmed that the transcription levels of *P. aeruginiosa gapA* and *zwf* were induced by a treatment with a steady dose of $H_2O_2$. The asterisks denote that the differences between $H_2O_2$-treated and untreated samples are statistically significant ($P < 0.05$). (C) Changes in metabolite levels in *P. aeruginosa* constitutively treated with and without 10 mM $H_2O_2$ for 10 min. Bacterial lysates were prepared, and metabolites were quantified by LC-MS/MS. The absolute metabolite concentrations were normalized and are presented as changes in percentage compared to the untreated control. (D) Gene organization in four glycolytic or ED operons of *P. aeruginosa*. HexR is the repressor for all the promoters. (E) The level of intracellular KDPG increased upon treatment with a steady dose of $H_2O_2$. The asterisks denote that the differences between $H_2O_2$-treated and untreated control (CK) samples are statistically significant ($P < 0.05$). (F) A *P. aeruginosa edd* mutant displayed a 4-fold-lower MIC to $H_2O_2$ than wild-type bacteria.

tion of KDPG (from 45 ± 15 to 150 ± 28 μM) (Fig. 5E), which suggests the importance of KDPG in response to ROS. Indeed, we found that an *edd* (which encodes phosphogluconate dehydratase that produces KDPG) mutant was 4-fold more sensitive to $H_2O_2$ (Fig. 5F), demonstrating that KDPG is a critical metabolite involved in resistance to ROS in *P. aeruginosa*.

We next purified a $His_6$-tagged full-length HexR protein that indeed strongly and specifically binds to the promoters of *zwf* and *gapA* in EMSA (Fig. 6A; see Fig. S3C in the supplemental material). Similar to the relationship between GapR and FBP in *S. aureus*, addition of 150 μM KDPG dissociates significantly more DNA from the HexR-DNA complex than does 50 μM KDPG (Fig. 6A). As a control, the HexR-DNA complexes are not sensitive to 10 mM $H_2O_2$. The subsequent DNase I footprint assay further confirmed two specific HexR-protected regions (−80 to −4 away from ATG) on the *zwf* promoter (Fig. 6B and C). Two putative HexR boxes ($TTGTN_6ACTA$, from −78 to −64, and $TTTGN_7ACAA$, from −18 to −4, respectively) (Fig. 6C) were located in these protected regions, which are very similar to the HexR motif ($TTGTN_{7-8}ACAA$) in *P. putida*. These two predicted putative

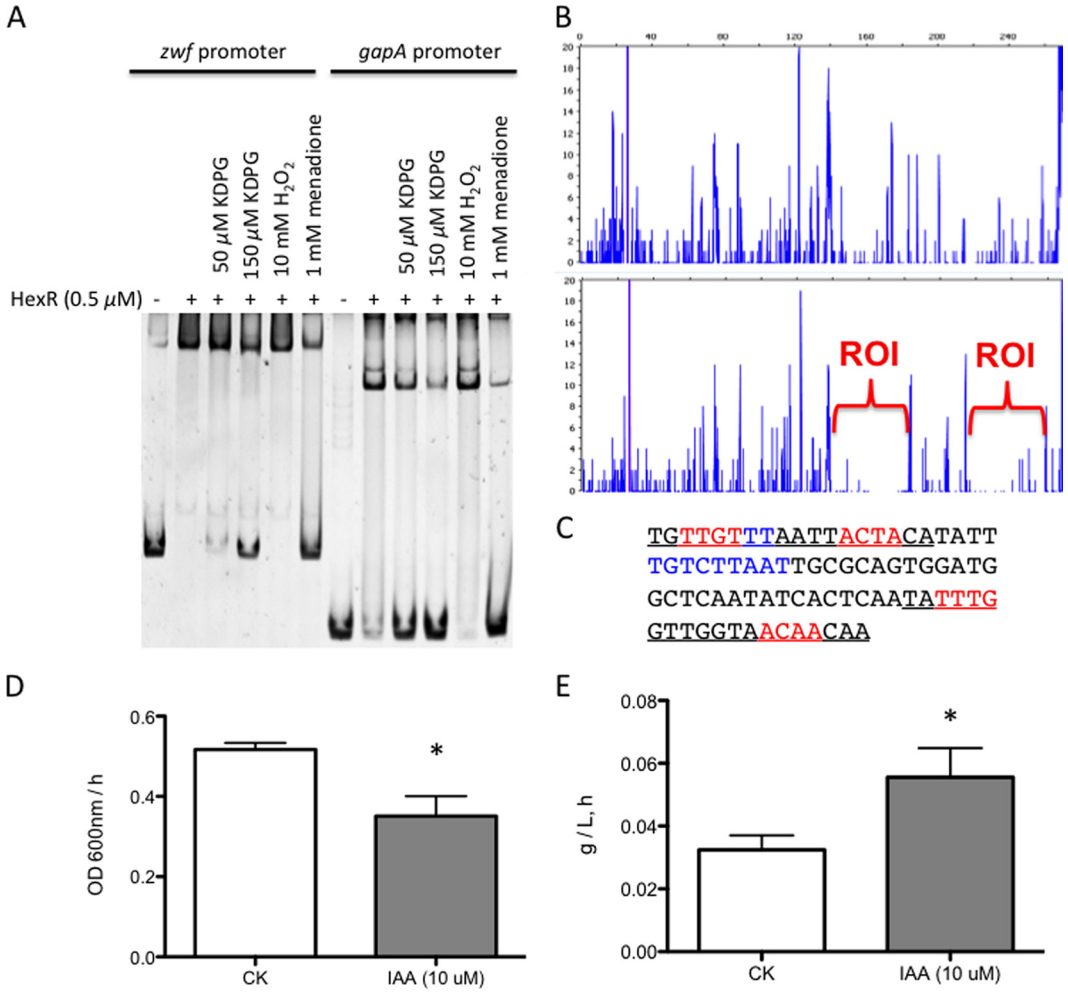


**FIG 6** 2-Keto-3-deoxy-6-phosphogluconate (KDPG) interacts with HexR and derepresses glycolytic genes in *P. aeruginosa*. (A) EMSA shows that HexR directly binds to the promoters of *zwf* and *gapA*. Addition of 150 μM KDPG dissociates significantly more DNA from the HexR-DNA complex than does 50 μM KDPG, which are the calculated *in vivo* concentrations after and before the steady dose of 10 mM $H_2O_2$. The protein-DNA complexes are not sensitive to 10 mM $H_2O_2$ but are sensitive to 1 mM menadione. (B) HexR directly binds to a HexR box-like motif in the *zwf* promoter according to a dye primer-based DNase I footprint assay. Electropherograms showing the protection pattern of the *gapR* promoter after digestion with DNase I following incubation in the absence (upper panel) or presence (lower panel) of 1 μM HexR. ROI, region of interest. (C) *zwf* promoter sequence (−80 from ATG) with a summary of the DNase I footprint assay results. The −35 and −10 promoter regions are highlighted in blue. The two HexR-protected regions are underlined, and the putative inverted repeats in the HexR motif are highlighted in red. (D) Supplementation with 400 μM iodoacetic acid (IAA) reduced the growth rate of *P. aeruginosa* in LB at the mid-log phase. CK, untreated control. (E) The rate of glucose uptake in *P. aeruginosa* increased upon treatment with 400 μM IAA. The asterisk denotes that the differences between IAA-treated and untreated samples are statistically significant ($P < 0.05$).

HexR boxes are located downstream of the −35 and −10 consensus sequences (highlighted in blue in Fig. 6C).

Since the steady-state levels of $H_2O_2$ induced both the gene expression and intracellular levels of metabolites in the glycolysis ED pathway, we reason that continuous treatment with $H_2O_2$ might boost the glucose uptake in *P. aeruginosa* as well. In order to test this hypothesis, the glucose uptake rates were calculated by measuring the concentration of the remaining glucose in the growth medium posttreatment with IAA for 1 h. Since $H_2O_2$ interfered with the measurement of glucose, IAA was used to mimic the inhibitory effect of GAPDH. Indeed, IAA significantly induced the glucose uptake rate, while inhibiting bacterial growth (Fig. 6D and E). On the other hand, GAPDH inhibition did not induce glucose uptake in *S. aureus* (data not shown). We noted that, unlike in *P. aeruginosa*, genes involved in glucose uptake in *S. aureus* (*glk*, *glcU*, and *glcA*) were not significantly induced under the steady-state level of $H_2O_2$, which could explain the discrepancy between the two bacteria (see Table S2 in the supplemental material).

## DISCUSSION

A key measure for bacteria to counteract oxidative damage is to maintain the intracellular redox state, which is mostly governed by ratios of NADH to $NAD^+$ and NADPH to $NADP^+$. NADH and NADPH fuel the antioxidant activities of alkyl hydroperoxidase and glutathione and thioredoxin reductases. NADH acts as a pro-oxidant that feeds reducing equivalents to flavoproteins (56). PPP is the major pathway for NADPH production, which raises the bacterial electrochemical potential that is involved in antioxidant tolerance. A similar role of GAPDH as a metabolic

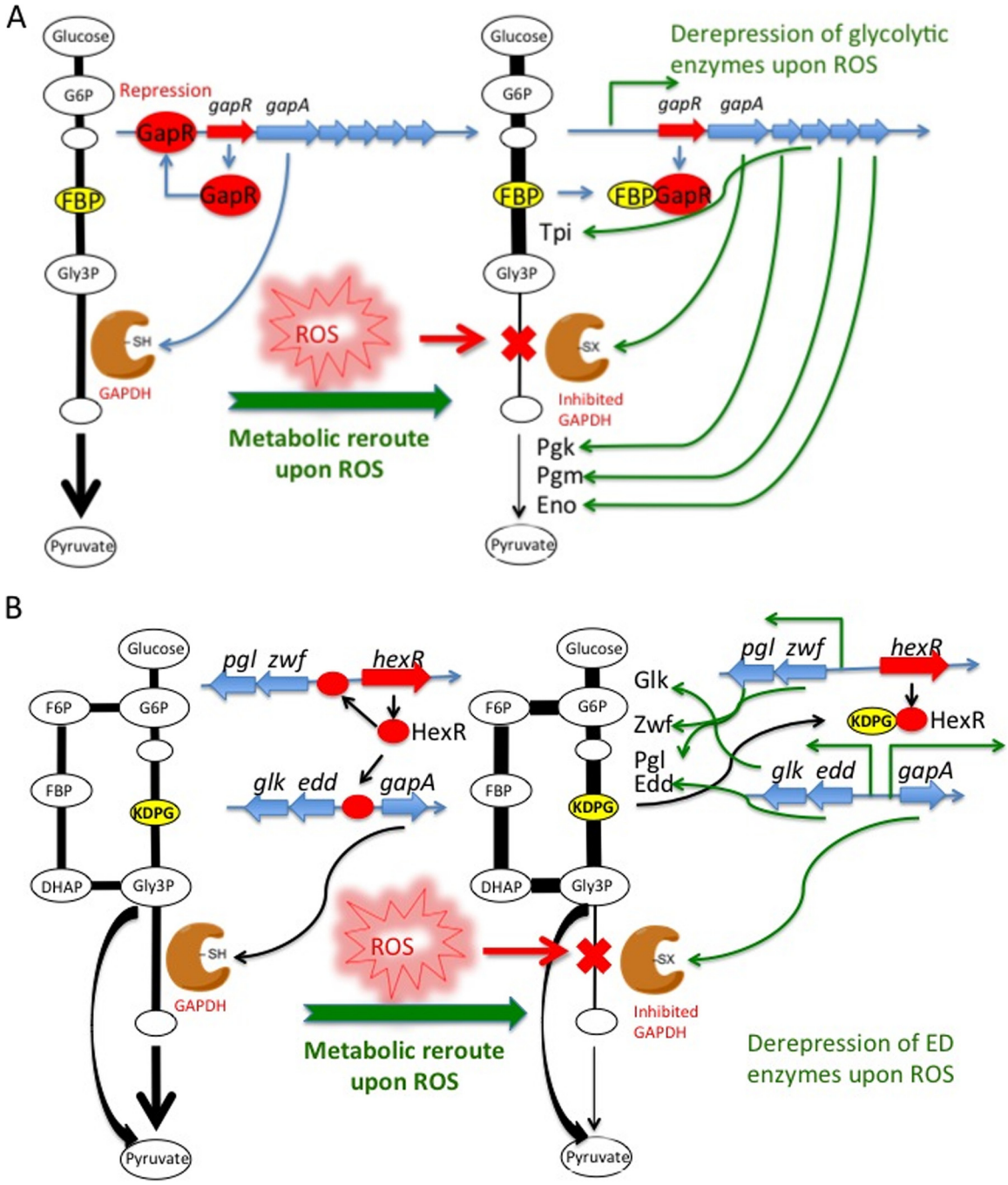


**FIG 7** Metabolite-mediated glycolytic derepression under steady-state treatment with $H_2O_2$. (A) In *S. aureus*, ROS inactivation of GAPDH leads to a metabolic reconfiguration from glycolysis to the pentose phosphate pathway, thus increasing the intracellular levels of FBP. Subsequently, elevated levels of FBP interact with the glycolytic repressor GapR, which leads to its dissociation from its own promoter. Finally, the glycolytic genes are derepressed. (B) In *P. aeruginosa*, the induced glycolysis increased the intracellular levels of KDPG, which binds to the glycolytic repressor HexR. KDPG-mediated release of HexR from the promoters of *gapA* and *zwf* results in the derepression of the glycolytic genes.

switch has been previously characterized in yeast, illustrating evolutionary conservation of this strategy in both prokaryotes and eukaryotes (25, 57). The altered levels of metabolites might also function as antioxidant signals. The steady-state level of $H_2O_2$ significantly induces a group of metabolic pathways, including fatty acid, tryptophan, and pyrimidine metabolism (Fig. 2), which could serve as a "sink" to dispose PPP intermediates and produce excess NADPH. In addition, $H_2O_2$ helps to consume NADPH that is responsible for GSH production. Moreover, we show that the inactivation of GAPDH decreases the intracellular NADH level that contributes to the proton motive force (PMF) and promotes the survival of bacterial persisters that are treated by aminoglycosides and glycolytic metabolites. Although this strategy is limited to only one category

of antibiotics, our findings imply that oxidative stress would be beneficial for persisters to escape killing.

Previously, we found that *P. aeruginosa* and *S. aureus* were able to largely degrade millimolar levels of $H_2O_2$ in several minutes in the mid-log-phase culture *in vitro* (16). However, inside the host, $H_2O_2$ can be produced constitutively by the immune response with steady doses (1), which suggests that $H_2O_2$ should be continuously supplemented *in vitro* in order to best mimic the physiological conditions under the host immune response. The rationale was validated by the observation of induced glycolysis inside these bacteria when challenged with a steady-state level of $H_2O_2$ but not the one-dose $H_2O_2$ treatment (Fig. 1A; see Fig. S1A in the supplemental material) commonly used in studying ROS sensing and response in bacteria (26). With this in mind, previous microarray analyses that are based on one-dose $H_2O_2$ treatment may not comprehensively represent the *in vivo* transcriptomic changes elicited by host-derived ROS (26, 27, 47). Therefore, we used a dialysis bag to continuously treat bacteria with 10 mM $H_2O_2$ before employing RNA-seq to globally profile transcriptional changes.

Interestingly, our present RNA-seq analyses uncovered that glycolytic genes were upregulated and significantly enriched for both tested bacteria. The subsequent biochemical and genetic characterizations demonstrated that following $H_2O_2$ inactivation of GAPDH, which induces glycolysis and PPP, the elevated levels of FBP and KDPG lead to dissociation of their corresponding glycolytic repressors (GapR and HexR, respectively) from the cognate promoters, thus resulting in derepression of the glycolytic genes to overcome $H_2O_2$-stalled glycolysis in *S. aureus* and *P. aeruginosa*, respectively (Fig. 7A and B). There is increasing evidence that metabolites are important in modulating glycolytic flux (58). The metabolite quantification further confirmed that the glycolysis is activated by the steady-state treatments with $H_2O_2$ for both pathogenic bacteria (Fig. 3C and 5C). This is reminiscent of the observation that *zwf* was found to be induced by oxidative stress in *Pseudomonas putida* (59). The similar ROS-induced glycolysis has been well documented in eukaryotic systems, including yeast and cancer cells (60, 61). The most intriguing example is the well-known Warburg effect, in which cancer cells have increased rates of glycolysis despite the presence of elevated $O_2$ and ROS levels; however, its underlying mechanism has yet to be completely revealed (62, 63).

Besides the direct derepression of GapR and HexR by FBP and KDPG, other mechanisms may also contribute to the induction of glycolytic genes in both pathogenic bacteria. In a previous study, 20 mM menadione, but not 500 mM $H_2O_2$, attenuated the DNA binding affinity of *P. putida* HexR, which suggests it could be a direct sensor of oxidative stress (59). We also demonstrated that 1 mM menadione can efficiently dissociate both GapR-DNA and HexR-DNA complexes (Fig. 4A and 6A). Given that exposure of bacteria to $H_2O_2$ tunes the menadiol-menadione equilibrium toward the oxidized form, menadione could be directly sensed by both GapR and HexR, thus leading to derepression of their corresponding glycolysis pathways. The direct interactions between them will be studied in the future.

In conclusion, different from previous microarray analyses that are based on one-dose treatment with $H_2O_2$, our metabolomic and transcriptomic profiling as well as subsequent biochemical and genetic characterizations demonstrated that steady-state stress of $H_2O_2$ induces glycolysis and PPP as well as profound transcriptional changes. Under steady-state stress of $H_2O_2$ that is produced by the host immune response, bacteria use different layers of mechanisms to counter ROS stress. First, the level of the major reductant NADPH is elevated following rapid inhibition of GAPDH by ROS. Second, metabolite-mediated transcriptional derepression overcomes the inhibition of GAPDH, thus leading to increased levels of glycolysis or the ED pathway (Fig. 7A and B). Finally, many more differently transcribed genes revealed from this study strongly suggest that additional ROS sensing and response mechanisms used by bacteria remain to be uncovered. The approach of integrating metabolomics into transcriptional regulation holds the potential for a comprehensive understanding of metabolic regulation by the host-derived steady state of ROS.

## ACKNOWLEDGMENTS

This work was supported by National Institutes of Health grants (AI074658 and P50GM081892 to C.H.) and a Burroughs Wellcome Fund Investigator in the Pathogenesis of Infectious Disease Award (to C.H.).

We are grateful to J. A. Morrissey at the University of Leicester for providing the *S. aureus gapA* and *gapR* deletion strains and Colin Manoil at the University of Washington for providing the *edd* mutant.

We declare that we have no conflicts of interest.

## REFERENCES

1. **Winterbourn CC, Hampton MB, Livesey JH, Kettle AJ.** 2006. Modeling the reactions of superoxide and myeloperoxidase in the neutrophil phagosome: implications for microbial killing. J. Biol. Chem. **281:**39860–39869. http://dx.doi.org/10.1074/jbc.M605898200.
2. **Hassett DJ, Cohen MS.** 1989. Bacterial adaptation to oxidative stress: implications for pathogenesis and interaction with phagocytic cells. FASEB J. **3:**2574–2582.
3. **Clauditz A, Resch A, Wieland KP, Peschel A, Gotz F.** 2006. Staphyloxanthin plays a role in the fitness of *Staphylococcus aureus* and its ability to cope with oxidative stress. Infect. Immun. **74:**4950–4953. http://dx.doi.org/10.1128/IAI.00204-06.
4. **delCardayre SB, Stock KP, Newton GL, Fahey RC, Davies JE.** 1998. Coenzyme A disulfide reductase, the primary low molecular weight disulfide reductase from *Staphylococcus aureus*. Purification and characterization of the native enzyme. J. Biol. Chem. **273:**5744–5751.
5. **Storz G, Imlay JA.** 1999. Oxidative stress. Curr. Opin. Microbiol. **2:**188–194. http://dx.doi.org/10.1016/S1369-5274(99)80033-2.
6. **Chen PR, Bae T, Williams WA, Duguid EM, Rice PA, Schneewind O, He C.** 2006. An oxidation-sensing mechanism is used by the global regulator MgrA in *Staphylococcus aureus*. Nat. Chem. Biol. **2:**591–595. http://dx.doi.org/10.1038/nchembio820.
7. **Fuangthong M, Helmann JD.** 2002. The OhrR repressor senses organic hydroperoxides by reversible formation of a cysteine-sulfenic acid derivative. Proc. Natl. Acad. Sci. U. S. A. **99:**6690–6695. http://dx.doi.org/10.1073/pnas.102483199.
8. **Fujimoto DF, Higginbotham RH, Sterba KM, Maleki SJ, Segall AM, Smeltzer MS, Hurlburt BK.** 2009. *Staphylococcus aureus* SarA is a regulatory protein responsive to redox and pH that can support bacteriophage lambda integrase-mediated excision/recombination. Mol. Microbiol. **74:**1445–1458. http://dx.doi.org/10.1111/j.1365-2958.2009.06942.x.
9. **Gaudu P, Weiss B.** 1996. SoxR, a [2Fe-2S] transcription factor, is active only in its oxidized form. Proc. Natl. Acad. Sci. U. S. A. **93:**10094–10098. http://dx.doi.org/10.1073/pnas.93.19.10094.
10. **Chen PR, Nishida S, Poor CB, Cheng A, Bae T, Kuechenmeister L, Dunman PM, Missiakas D, He C.** 2009. A new oxidative sensing and regulation pathway mediated by the MgrA homologue SarZ in *Staphylococcus aureus*. Mol. Microbiol. **71:**198–211. http://dx.doi.org/10.1111/j.1365-2958.2008.06518.x.
11. **Chen H, Hu J, Chen PR, Lan L, Li Z, Hicks LM, Dinner AR, He C.** 2008. The *Pseudomonas aeruginosa* multidrug efflux regulator MexR uses an oxidation-sensing mechanism. Proc. Natl. Acad. Sci. U. S. A. **105:**13586–13591. http://dx.doi.org/10.1073/pnas.0803391105.
12. **Sun F, Ji Q, Jones MB, Deng X, Liang H, Frank B, Telser J, Peterson SN, Bae T, He C.** 2012. AirSR, a [2Fe-2S] cluster-containing two-component

system, mediates global oxygen sensing and redox signaling in *Staphylococcus aureus*. J. Am. Chem. Soc. **134:**305–314. http://dx.doi.org/10.1021/ja2071835.
13. **Sun F, Liang H, Kong X, Xie S, Cho H, Deng X, Ji Q, Zhang H, Alvarez S, Hicks LM, Bae T, Luo C, Jiang H, He C.** 2012. Quorum-sensing *agr* mediates bacterial oxidation response via an intramolecular disulfide redox switch in the response regulator AgrA. Proc. Natl. Acad. Sci. U. S. A. **109:**9095–9100. http://dx.doi.org/10.1073/pnas.1200603109.
14. **Ji Q, Zhang L, Sun F, Deng X, Liang H, Bae T, He C.** 2012. *Staphylococcus aureus* CymR is a new thiol-based oxidation-sensing regulator of stress resistance and oxidative response. J. Biol. Chem. **287:**21102–21109. http://dx.doi.org/10.1074/jbc.M112.359737.
15. **Lan L, Murray TS, Kazmierczak BI, He C.** 2010. *Pseudomonas aeruginosa* OspR is an oxidative stress sensing regulator that affects pigment production, antibiotic resistance and dissemination during infection. Mol. Microbiol. **75:**76–91. http://dx.doi.org/10.1111/j.1365-2958.2009.06955.x.
16. **Deng X, Weerapana E, Ulanovskaya O, Sun F, Liang H, Ji Q, Ye Y, Fu Y, Zhou L, Li J, Zhang H, Wang C, Alvarez S, Hicks LM, Lan L, Wu M, Cravatt BF, He C.** 2013. Proteome-wide quantification and characterization of oxidation-sensitive cysteines in pathogenic bacteria. Cell Host Microbe **13:**358–370. http://dx.doi.org/10.1016/j.chom.2013.02.004.
17. **Chen PR, Brugarolas P, He C.** 2011. Redox signaling in human pathogens. Antioxid. Redox Signal. **14:**1107–1118. http://dx.doi.org/10.1089/ars.2010.3374.
18. **Kruger A, Gruning NM, Wamelink MM, Kerick M, Kirpy A, Parkhomchuk D, Bluemlein K, Schweiger MR, Soldatov A, Lehrach H, Jakobs C, Ralser M.** 2011. The pentose phosphate pathway is a metabolic redox sensor and regulates transcription during the antioxidant response. Antioxid. Redox Signal. **15:**311–324. http://dx.doi.org/10.1089/ars.2010.3797.
19. **Perry AC, Ni Bhriain N, Brown NL, Rouch DA.** 1991. Molecular characterization of the *gor* gene encoding glutathione reductase from *Pseudomonas aeruginosa*: determinants of substrate specificity among pyridine nucleotide-disulphide oxidoreductases. Mol. Microbiol. **5:**163–171. http://dx.doi.org/10.1111/j.1365-2958.1991.tb01837.x.
20. **Uziel O, Borovok I, Schreiber R, Cohen G, Aharonowitz Y.** 2004. Transcriptional regulation of the *Staphylococcus aureus* thioredoxin and thioredoxin reductase genes in response to oxygen and disulfide stress. J. Bacteriol. **186:**326–334. http://dx.doi.org/10.1128/JB.186.2.326-334.2004.
21. **Zhang YM, Liu JK, Wong TY.** 2003. The DNA excision repair system of the highly radioresistant bacterium *Deinococcus radiodurans* is facilitated by the pentose phosphate pathway. Mol. Microbiol. **48:**1317–1323. http://dx.doi.org/10.1046/j.1365-2958.2003.03486.x.
22. **Purves J, Cockayne A, Moody PC, Morrissey JA.** 2010. Comparison of the regulation, metabolic functions, and roles in virulence of the glyceraldehyde-3-phosphate dehydrogenase homologues *gapA* and *gapB* in *Staphylococcus aureus*. Infect. Immun. **78:**5223–5232. http://dx.doi.org/10.1128/IAI.00762-10.
23. **Doan T, Aymerich S.** 2003. Regulation of the central glycolytic genes in *Bacillus subtilis*: binding of the repressor CggR to its single DNA target sequence is modulated by fructose-1,6-bisphosphate. Mol. Microbiol. **47:**1709–1721. http://dx.doi.org/10.1046/j.1365-2958.2003.03404.x.
24. **Daddaoua A, Krell T, Ramos JL.** 2009. Regulation of glucose metabolism in *Pseudomonas*: the phosphorylative branch and Entner-Doudoroff enzymes are regulated by a repressor containing a sugar isomerase domain. J. Biol. Chem. **284:**21360–21368. http://dx.doi.org/10.1074/jbc.M109.014555.
25. **Ralser M, Wamelink MM, Kowald A, Gerisch B, Heeren G, Struys EA, Klipp E, Jakobs C, Breitenbach M, Lehrach H, Krobitsch S.** 2007. Dynamic rerouting of the carbohydrate flux is key to counteracting oxidative stress. J. Biol. **6:**10. http://dx.doi.org/10.1186/jbiol61.
26. **Chang W, Small DA, Toghrol F, Bentley WE.** 2006. Global transcriptome analysis of *Staphylococcus aureus* response to hydrogen peroxide. J. Bacteriol. **188:**1648–1659. http://dx.doi.org/10.1128/JB.188.4.1648-1659.2006.
27. **Chang W, Small DA, Toghrol F, Bentley WE.** 2005. Microarray analysis of *Pseudomonas aeruginosa* reveals induction of pyocin genes in response to hydrogen peroxide. BMC Genomics **6:**115. http://dx.doi.org/10.1186/1471-2164-6-115.
28. **Meyer H, Liebeke M, Lalk M.** 2010. A protocol for the investigation of the intracellular *Staphylococcus aureus* metabolome. Anal. Biochem. **401:**250–259. http://dx.doi.org/10.1016/j.ab.2010.03.003.
29. **Kopp F, Komatsu T, Nomura DK, Trauger SA, Thomas JR, Siuzdak G, Simon GM, Cravatt BF.** 2010. The glycerophospho metabolome and its influence on amino acid homeostasis revealed by brain metabolomics of GDE1(−/−) mice. Chem. Biol. **17:**831–840. http://dx.doi.org/10.1016/j.chembiol.2010.06.009.
30. **Trapnell C, Pachter L, Salzberg SL.** 2009. TopHat: discovering splice junctions with RNA-Seq. Bioinformatics **25:**1105–1111. http://dx.doi.org/10.1093/bioinformatics/btp120.
31. **Trapnell C, Williams BA, Pertea G, Mortazavi A, Kwan G, van Baren MJ, Salzberg SL, Wold BJ, Pachter L.** 2010. Transcript assembly and quantification by RNA-Seq reveals unannotated transcripts and isoform switching during cell differentiation. Nat. Biotechnol. **28:**511–515. http://dx.doi.org/10.1038/nbt.1621.
32. **Huang DW, Sherman BT, Lempicki RA.** 2009. Systematic and integrative analysis of large gene lists using DAVID bioinformatics resources. Nat. Protoc. **4:**44–57. http://dx.doi.org/10.1038/nprot.2008.211.
33. **Saito R, Smoot ME, Ono K, Ruscheinski J, Wang PL, Lotia S, Pico AR, Bader GD, Ideker T.** 2012. A travel guide to Cytoscape plugins. Nat. Methods **9:**1069–1076. http://dx.doi.org/10.1038/nmeth.2212.
34. **National Committee for Clinical Laboratory Standards.** 2000. Methods for dilution antimicrobial susceptibility tests for bacteria that grow aerobically—5th ed: approved standard M7-A5. NCCLS, Wayne, PA.
35. **Jin Q, Thilmony R, Zwiesler-Vollick J, He SY.** 2003. Type III protein secretion in *Pseudomonas syringae*. Microbes Infect. **5:**301–310. http://dx.doi.org/10.1016/S1286-4579(03)00032-7.
36. **Donnelly MI, Zhou M, Millard CS, Clancy S, Stols L, Eschenfeldt WH, Collart FR, Joachimiak A.** 2006. An expression vector tailored for large-scale, high-throughput purification of recombinant proteins. Protein Expr. Purif. **47:**446–454. http://dx.doi.org/10.1016/j.pep.2005.12.011.
37. **Zianni M, Tessanne K, Merighi M, Laguna R, Tabita FR.** 2006. Identification of the DNA bases of a DNase I footprint by the use of dye primer sequencing on an automated capillary DNA analysis instrument. J. Biomol. Tech. **17:**103–113.
38. **Allison KR, Brynildsen MP, Collins JJ.** 2011. Metabolite-enabled eradication of bacterial persisters by aminoglycosides. Nature **473:**216–220. http://dx.doi.org/10.1038/nature10069.
39. **Bergmeyer HU, Bergmeyer J, Grassl M.** 1983. Methods of enzymatic analysis, 3rd ed. Verlag Chemie, Weinheim, Germany.
40. **Cook GA, O'Brien WE, Wood HG, King MT, Veech RL.** 1978. A rapid, enzymatic assay for the measurement of inorganic pyrophosphate in animal tissues. Anal. Biochem. **91:**557–565. http://dx.doi.org/10.1016/0003-2697(78)90543-2.
41. **Yuroff AS, Sabat G, Hickey WJ.** 2003. Transporter-mediated uptake of 2-chloro- and 2-hydroxybenzoate by *Pseudomonas huttiensis* strain D1. Appl. Environ. Microbiol. **69:**7401–7408. http://dx.doi.org/10.1128/AEM.69.12.7401-7408.2003.
42. **Cheriyan M, Toone EJ, Fierke CA.** 2007. Mutagenesis of the phosphate-binding pocket of KDPG aldolase enhances selectivity for hydrophobic substrates. Protein Sci. **16:**2368–2377. http://dx.doi.org/10.1110/ps.073042907.
43. **Hoang TT, Karkhoff-Schweizer RR, Kutchma AJ, Schweizer HP.** 1998. A broad-host-range Flp-FRT recombination system for site-specific excision of chromosomally-located DNA sequences: application for isolation of unmarked *Pseudomonas aeruginosa* mutants. Gene **212:**77–86. http://dx.doi.org/10.1016/S0378-1119(98)00130-9.
44. **Kirsch M, De Groot H.** 2001. NAD(P)H, a directly operating antioxidant? FASEB J. **15:**1569–1574. http://dx.doi.org/10.1096/fj.00-0823hyp.
45. **Poolman B, Bosman B, Kiers J, Konings WN.** 1987. Control of glycolysis by glyceraldehyde-3-phosphate dehydrogenase in *Streptococcus cremoris* and *Streptococcus lactis*. J. Bacteriol. **169:**5887–5890.
46. **Korshunov SS, Imlay JA.** 2002. A potential role for periplasmic superoxide dismutase in blocking the penetration of external superoxide into the cytosol of Gram-negative bacteria. Mol. Microbiol. **43:**95–106. http://dx.doi.org/10.1046/j.1365-2958.2002.02719.x.
47. **Palma M, DeLuca D, Worgall S, Quadri LE.** 2004. Transcriptome analysis of the response of *Pseudomonas aeruginosa* to hydrogen peroxide. J. Bacteriol. **186:**248–252. http://dx.doi.org/10.1128/JB.186.1.248-252.2004.
48. **Salunkhe P, Topfer T, Buer J, Tummler B.** 2005. Genome-wide transcriptional profiling of the steady-state response of *Pseudomonas aeruginosa* to hydrogen peroxide. J. Bacteriol. **187:**2565–2572. http://dx.doi.org/10.1128/JB.187.8.2565-2572.2005.
49. **Wolf C, Hochgrafe F, Kusch H, Albrecht D, Hecker M, Engelmann S.** 2008. Proteomic analysis of antioxidant strategies of *Staphylococcus au-*

*reus*: diverse responses to different oxidants. Proteomics **8:**3139–3153. http://dx.doi.org/10.1002/pmic.200701062.

50. **Juhas M, Wiehlmann L, Huber B, Jordan D, Lauber J, Salunkhe P, Limpert AS, von Gotz F, Steinmetz I, Eberl L, Tummler B.** 2004. Global regulation of quorum sensing and virulence by VqsR in *Pseudomonas aeruginosa*. Microbiology **150:**831–841. http://dx.doi.org/10.1099/mic.0.26906-0.
51. **Wurtzel O, Yoder-Himes DR, Han K, Dandekar AA, Edelheit S, Greenberg EP, Sorek R, Lory S.** 2012. The single-nucleotide resolution transcriptome of *Pseudomonas aeruginosa* grown in body temperature. PLoS Pathog. **8:**e1002945. http://dx.doi.org/10.1371/journal.ppat.1002945.
52. **Bennett BD, Kimball EH, Gao M, Osterhout R, Van Dien SJ, Rabinowitz JD.** 2009. Absolute metabolite concentrations and implied enzyme active site occupancy in Escherichia coli. Nat. Chem. Biol. **5:**593–599. http://dx.doi.org/10.1038/nchembio.186.
53. **Bijlsma JJ, Groisman EA.** 2003. Making informed decisions: regulatory interactions between two-component systems. Trends Microbiol. **11:**359–366. http://dx.doi.org/10.1016/S0966-842X(03)00176-8.
54. **Seidel G, Diel M, Fuchsbauer N, Hillen W.** 2005. Quantitative interdependence of coeffectors, CcpA and cre in carbon catabolite regulation of *Bacillus subtilis*. FEBS J. **272:**2566–2577. http://dx.doi.org/10.1111/j.1742-4658.2005.04682.x.
55. **Petruschka L, Adolf K, Burchhardt G, Dernedde J, Jurgensen J, Herrmann H.** 2002. Analysis of the *zwf-pgl-eda*-operon in *Pseudomonas putida* strains H and KT2440. FEMS Microbiol. Lett. **215:**89–95. http://dx.doi.org/10.1111/j.1574-6968.2002.tb11375.x.
56. **Henard CA, Bourret TJ, Song M, Vazquez-Torres A.** 2010. Control of redox balance by the stringent response regulatory protein promotes antioxidant defenses of *Salmonella*. J. Biol. Chem. **285:**36785–36793. http://dx.doi.org/10.1074/jbc.M110.160960.
57. **Ralser M, Wamelink MM, Latkolik S, Jansen EE, Lehrach H, Jakobs C.** 2009. Metabolic reconfiguration precedes transcriptional regulation in the antioxidant response. Nat. Biotechnol. **27:**604–605. http://dx.doi.org/10.1038/nbt0709-604.
58. **Doucette CD, Schwab DJ, Wingreen NS, Rabinowitz JD.** 2011. α-Ketoglutarate coordinates carbon and nitrogen utilization via enzyme I inhibition. Nat. Chem. Biol. **7:**894–901. http://dx.doi.org/10.1038/nchembio.685.
59. **Kim J, Jeon CO, Park W.** 2008. Dual regulation of *zwf-1* by both 2-keto-3-deoxy-6-phosphogluconate and oxidative stress in *Pseudomonas putida*. Microbiology **154:**3905–3916. http://dx.doi.org/10.1099/mic.0.2008/020362-0.
60. **Chechik G, Oh E, Rando O, Weissman J, Regev A, Koller D.** 2008. Activity motifs reveal principles of timing in transcriptional control of the yeast metabolic network. Nat. Biotechnol. **26:**1251–1259. http://dx.doi.org/10.1038/nbt.1499.
61. **Warburg O.** 1956. On the origin of cancer cells. Science **123:**309–314. http://dx.doi.org/10.1126/science.123.3191.309.
62. **Gatenby RA, Gillies RJ.** 2004. Why do cancers have high aerobic glycolysis? Nat. Rev. Cancer **4:**891–899. http://dx.doi.org/10.1038/nrc1478.
63. **Kim JW, Dang CV.** 2006. Cancer's molecular sweet tooth and the Warburg effect. Cancer Res. **66:**8927–8930. http://dx.doi.org/10.1158/0008-5472.CAN-06-1501.